

See discussions, stats, and author profiles for this publication at: <https://www.researchgate.net/publication/263550269>

# The Trifluoromethyl Group as a Conformational Stabilizer and Probe: Conformational Analysis of Cinchona Alkaloid Scaffolds

ARTICLE *in* JOURNAL OF THE AMERICAN CHEMICAL SOCIETY · JUNE 2014

Impact Factor: 12.11 · DOI: 10.1021/ja504376u · Source: PubMed

---

CITATIONS

5

---

READS

36

7 AUTHORS, INCLUDING:



Fang Wang

Massachusetts Institute of Technology

32 PUBLICATIONS 410 CITATIONS

SEE PROFILE



Zhe Zhang

University of Southern California

12 PUBLICATIONS 106 CITATIONS

SEE PROFILE

# The Trifluoromethyl Group as a Conformational Stabilizer and Probe: Conformational Analysis of Cinchona Alkaloid Scaffolds

G. K. Surya Prakash,\* Fang Wang, Martin Rahm, Zhe Zhang, Chuanfa Ni, Jingguo Shen, George A. Olah

Loker Hydrocarbon Research Institute, Department of Chemistry, University of Southern California, Los Angeles, California 90089

## Supporting Information Placeholder

**ABSTRACT:** The introduction of the CF<sub>3</sub> group on the C9 atom in quinidine can significantly increase the conformational interconversion barrier of the cinchona alkaloid scaffold. With this modification the conformational behavior of cinchona alkaloids in various solvents can be conveniently investigated via <sup>19</sup>F NMR spectroscopy. Based on the reliable conformational distribution information obtained, the accuracy of both theoretical (PCM) and empirical (Kamlet-Taft) solvation models has been assessed using linear free energy relationship methods. The empirical solvation model was found to provide accurate prediction of solvent effects, while PCM demonstrated a relatively low reliability in the present study. Utilizing similar empirical solvation models along with Karplus-type equations, the conformational behavior of quinidine and 9-*epi*quinidine has also been investigated. A model S<sub>N</sub>2 reaction has been presented to reveal the important role of solvent-induced conformational behavior of cinchona alkaloids in their reactivity.

## INTRODUCTION

Cinchona alkaloid-based catalysts are privileged chiral scaffolds in asymmetric catalysis.<sup>1</sup> In an effort to improve their catalytic efficacy, in-depth mechanistic insight has been ardently sought. Among various factors, the conformations of catalysts have long been proposed to play a pivotal role in cinchona alkaloid-based catalysis.<sup>2</sup> Although this hypothesis has been invoked by both experiments<sup>3,4,5,6,7</sup> and theory,<sup>8</sup> the conformational behavior of cinchona alkaloids is still not thoroughly understood due to its capricious nature.

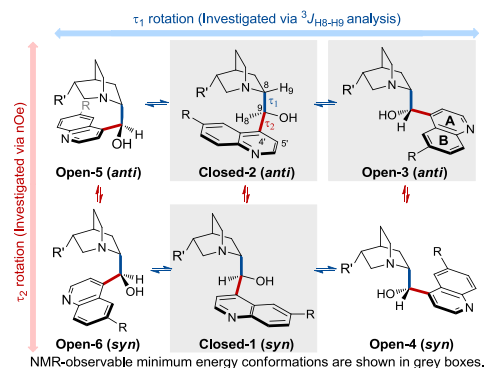
Pioneering studies by Dijkstra, Wynberg, and Sharpless have shown that the substantial fluxionality of cinchona alkaloids arises from rotations around the C8-C9 and C4'-C9 bonds ( $\tau_1$  and  $\tau_2$ , respectively, Scheme 1).<sup>3</sup> The  $\tau_1$  rotation leads to the interconversion of Closed and Open conformations, in which the quinuclidine nitrogen points to and away from Ring A of quinoline, respectively. Through the  $\tau_2$  rotation, *syn* and *anti* conformations are generated, as differentiated by the relative orientation of the -OH group aligning along and apart from Ring B of the quinoline moiety, respectively.

Detailed studies by Baiker,<sup>5,9</sup> Zeara,<sup>10</sup> and others<sup>7a,11</sup> have revealed that the conformational behavior of cinchona alkaloids could be significantly influenced by various intermolecular forces, such as dipole-dipole interactions, hydrogen bonding interactions,

and protonation on the quinuclidine nitrogen. Due to the complicated conformational scenario, multiple techniques are required for conformational studies of cinchona alkaloids.

Among various means, quantum chemical calculations have been extensively used to provide precise descriptions of three-dimensional structures of conformers. Three predominant minimum energy species have been identified in the gas phase, namely the Open-3, the Closed-1, and the Closed-2 conformers (Scheme 1).<sup>3,12</sup> Energy calculations of conformers in solution are usually performed with an implicit consideration of solvent molecules. However, since cinchona alkaloids can interact with solvents via H-bonding, the accuracy of such calculations can be limited.<sup>13</sup>

## Scheme 1. Six Possible Conformations of Cinchona Alkaloids Generated via Rotations around $\tau_1$ and $\tau_2$ .



In comparison, NMR spectroscopic techniques have been widely applied in liquid phase conformational analyses. Since theoretical studies have found that conformers Closed-1 and Closed-2 are very similar in  $\phi_{H8C9C8H9}$  dihedral angles,<sup>5</sup> Closed-1 and Closed-2 conformations are expected to have practically the same <sup>3</sup>J<sub>H8H9</sub> coupling constant.<sup>14</sup> Hence, the Open-Closed equilibrium can be quantified via the <sup>3</sup>J<sub>H8H9</sub> coupling analysis using the following two-variable-two-equation system,<sup>5</sup>

$$J_{H8H9}^{obs} = J_{H8H9}^{Open-3} \times Pop_{Open-3} + J_{H8H9}^{Closed} \times Pop_{Closed} \quad Eq. 1$$

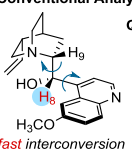
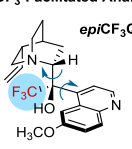
$$Pop_{Open-3} + Pop_{Closed} = 100\% \quad Eq. 2$$

wherein  $J_{H8H9}^{obs}$  is the observed  $J_{H8H9}$ , and  $J_{H8H9}^{Open-3}$  and  $J_{H8H9}^{Closed}$  are  $J_{H8H9}$  of Open-3 conformation and Closed conformations, respectively.  $Pop_{Open-3}$  and  $Pop_{Closed}$  are the populations of Open-3 conformation and Closed conformations, respectively. Since the conformational equilibrium was indirectly determined

based on Karplus-type correlations<sup>14</sup> with the exclusion of minor conformers, systematic errors are expected (Scheme 2).

In contrast to the relatively well studied  $\tau_1$  rotation, the  $\tau_2$  rotation has been rarely explored due to the absence of the corresponding vicinal protons. Even though nuclear Overhauser enhancement (nOe) spectroscopy can deliver information on  $\tau_2$  qualitatively, its accuracy in the quantification of conformational equilibria is under debate (Scheme 2).<sup>15</sup> In practice, systematic conformational studies on cinchona alkaloids have also been obstructed by the availability of deuterated solvents, which are necessary in most of the above mentioned NMR experiments (Scheme 2). The conformational study of cinchona alkaloids in liquid media has thus remained challenging because of (a) the difficulty in obtaining accurate experimental conformational distribution data, (b) the limited reliability of quantum chemical calculations, and (c) the lack of coherent studies of solvent effects on the conformational behavior of cinchona alkaloids.

**Scheme 2. Comparison of conventional cinchona alkaloid conformational analysis and the present trifluoromethyl-conformational stabilizing/probing strategy.**

Conventional Analysis	Analytical Tools	Possible errors/Problems
 <p>QD</p> <p>fast interconversion</p>	<sup>1</sup> H NMR Karplus-type equations nOe spectroscopy theoretical calculations	deuterated solvents required exclusion of minor conformers; accuracy of Karplus correlation semi-quantitative accuracy of solvation model
CF <sub>3</sub> -Facilitated Analysis	Analytical Tools	Possible errors/Advantages
 <p><i>epi</i>CF<sub>3</sub>QD</p> <p>slow interconversion</p>	the CF <sub>3</sub> group <sup>19</sup> F NMR nOe spectroscopy theoretical calculations	increase steric hindrance around C9 atom; weakly coordinating applicable in most solvents; direct measurement of conformational distribution only employed for qualitative conformational analysis accuracy can be assessed based on <sup>19</sup> F NMR data

Addressing such inherent challenges, we recently demonstrated that the sterically bulky CF<sub>3</sub> group<sup>16</sup> could be incorporated into the C9 atom in quinidine as a conformational stabilizer and a probe (Scheme 2).<sup>17</sup> The mechanistic basis underlying this protocol is the significantly increased barrier to the  $\tau_2$  rotation, which leads to the decoalescence of the signals of the *syn* and the *anti* conformations in both <sup>1</sup>H and <sup>19</sup>F NMR spectra at room temperature. The determination of the corresponding conformational equilibria is thus enabled by <sup>19</sup>F NMR peak integration.<sup>18</sup> This direct analytical protocol is not only more precise than the vicinal coupling constant analysis or 2D nOe spectroscopy, but also applicable in both deuterated and non-deuterated solvents (Scheme 2). With this protocol, a more diverse selection of solvents could be applied for a systematic investigation of solvent effects. Based on the accurate conformational information thus obtained, possible errors in energy calculations can be assessed (Scheme 2). Since H-bonding moieties (the hydroxyl and the amino groups) remain intact in the trifluoromethylated analogue (*epi*CF<sub>3</sub>QD), various specific solvent-solute interactions are expected to be relatively unperturbed. More importantly, due to its weakly interacting nature, the CF<sub>3</sub> group, although bulky, should only introduce negligible specific interactions to solvents. Thus, the environmental dependence of the conformations of *epi*CF<sub>3</sub>QD is anticipated to largely reflect that of naturally occurring cinchona alkaloids, and the conformational behavior of the latter can be investigated using a similar protocol. Based on the above mentioned method, reliable cinchona alkaloid conformational distributions in solution can be obtained, which are informative for the elucidation of active conformations in chemical reactions.

In this article, we quantitatively analyze the solvent dependence of the conformational behavior of cinchona alkaloids, which is primarily facilitated by a combination of NMR studies and DFT

calculations. Initially, we have performed the DFT calculations on quinidine (QD) and its derivatives. The first section (Section 2.1) is organized as (a) DFT calculations of the geometry of conformers of cinchona alkaloids and their derivatives, such as *epi*CF<sub>3</sub>QD, QD and 9-*epi*quinidine (*epi*QD); (b) DFT calculations of the relative energies of these conformers and the corresponding conformational distribution in the gas phase and in solution. In the second section, we describe the quantitative assessment of the reliability of quantum chemical calculation based on the accurate conformational information of *epi*CF<sub>3</sub>QD obtained from <sup>19</sup>F NMR spectroscopy. Section 2.2 describes (a) determination of the *syn-anti* conformational distribution of *epi*CF<sub>3</sub>QD in various solvents via <sup>19</sup>F NMR spectroscopy; (b) systematic analysis of solvent effects on *epi*CF<sub>3</sub>QD conformational behavior based on linear free energy relationship (LFER); (c) assessment of the accuracy of the quantum chemical calculation by comparing calculated conformational distribution of *epi*CF<sub>3</sub>QD with experimental outcomes. This section leads to the conclusion that the small solvation energy difference of conformers cannot be adequately predicted by implicit solvation models, such as the polarizable continuum model (PCM) commonly used in cinchona alkaloid conformational studies. This is primarily due to the inaccurate description of specific solvent-solute interactions by the PCM.

In Section 2.3, we discuss the solvent-dependent conformational behavior of *epi*QD. This section involves: (a) determination of the Open-Closed conformational distribution of *epi*QD in various solvents via <sup>1</sup>H NMR spectroscopy and Karplus-type analysis; (b) analysis of solvent effects on *epi*QD conformational behavior based on LFER; (c) assessment of quantum chemical calculations based on experimental data, which demonstrates that conformers with >3.5 kcal/mol relative energies in the gas phase are unlikely to be populated in solution.

Section 2.4 is focused on (a) determination of the Open-Closed conformational distribution of QD in solution via <sup>1</sup>H NMR spectroscopy and Karplus-type analysis; (b) systematic analysis of solvent effects on QD conformational behavior based on LFER; (c) quantitative evaluation of the calculated conformational behavior of QD in solution, showing that PCM may not be suitable for conformational study of QD.

In the last section, a case study demonstrates that the reactivity of QD in a model S<sub>N</sub>2 reaction can be significantly affected by solvent-induced conformation changes, implying a pivotal role for conformational behavior of cinchona alkaloids in related reactions.

## Methods

### (a) Identification of Conformers via DFT Calculations

The conformations of cinchona alkaloid scaffolds are primarily determined by two critical rotations  $\tau_1$  and  $\tau_2$  (Figure 1-A). To identify the major conformations of a given cinchona alkaloid derivative, a potential energy surface (PES) as a function of  $\tau_1$  and  $\tau_2$  was calculated at the B3LYP/6-31+G(d) level in the gas phase using Gaussian 09.<sup>19</sup> The dihedral angles of the two rotations were systematically varied from 0° to 360° by an increment of 10°. The obtained conformations were further optimized over five steps for each constrained dihedral angles.<sup>20</sup> The conformational profile was formed as a 36×36 PES with 1296 geometry optimizations, revealing a series of conformations (numbered similarly to the previous report by Baiker, Figure 1-B and 1-C).<sup>9d</sup> Based on these structures, further refinement was performed at the B3LYP/6-311+G(d,p) level in the gas phase, which led to very small geometric changes.

In addition to the  $\tau_1$  and the  $\tau_2$  rotations, two more rotations,  $\tau_3$  and  $\tau_4$ , were also taken into consideration as they could result in the formation of intramolecular H-bonding and/or significant change in the dipole moment of conformers. Our theoretical cal-

culations showed that **1'**-like conformers are approximately 1 kcal/mol higher in energy than **1** in the gas phase (Figure 1-A). Similar results were obtained in the liquid phase by NOESY spectroscopy, in which only **1**-like conformations were detected. Based on these results, **1'** was not considered for further calculations. As  $\tau_3$  has three minima around its rotational axis, the number of possible conformations identified on the PES tripled. The additional conformers due to the  $\tau_3$  rotation were also optimized at the B3LYP/6-311+G(d,p) level in the gas phase. Since  $\tau_1$  and  $\tau_2$  angles were essentially unchanged upon the  $\tau_3$  rotation, the conformers generated due to the  $\tau_3$  rotation were differentiated by alphabetic appendices (such as Closed-1a, Closed-1b, and Closed-1c, Figure 1-A). In other words, for a given molecule, the conformers with the same numerical name have similar  $\tau_1$  and  $\tau_2$  values (however, for different molecules, the same numerical name may not indicate similar  $\tau_1$  and  $\tau_2$  values).

### (b) Energy Calculation and Population Distribution

To obtain accurate estimates of each conformer's energy, single point energies were calculated at the M06-2X/6-311+G(d,p)//B3LYP/6-311+G(d,p) level of theory. The hybrid meta exchange-correlation density functional M06-2X empirically accounts for dispersive interactions and has demonstrated high accuracy in main-group thermochemistry.<sup>21</sup> Solvent effects were included implicitly through the self-consistent reaction field approach, as implemented in the default PCM model in Gaussian 09.<sup>22,23</sup> Thermal and entropic corrections for both gas-phase and PCM-optimized structures were obtained by frequency analysis at the B3LYP/6-311+G(d,p) level in the gas phase. The frequency analyses also confirmed that all considered structures were true minima on the PES.

The relative population of each conformer at 298 K was derived using the Boltzmann equation. Herein,  $\Delta G_{\text{syn,cal}}$  is defined as the free energy corresponding to the difference between the calculated *syn* population relative to the calculated *anti* population,

$$\Delta G_{\text{syn,cal}} = -RT \ln(n\text{Pop}_{\text{syn}} / n\text{Pop}_{\text{anti}}). \quad \text{Eq. 3}$$

$\Delta G_{\text{open,cal}}$  is similarly defined as,

$$\Delta G_{\text{open,cal}} = -RT \ln(n\text{Pop}_{\text{open}} / n\text{Pop}_{\text{closed}}). \quad \text{Eq. 4}$$

Intramolecular H-bonding interactions were investigated by second order perturbation analysis of NBO orbitals.<sup>24</sup> The NBO framework ascribes charge transfer as the major contributor to H-bonding, and enables comparison between relevant quinuclidine- $N\text{TCO}_\text{H}^*$  interaction energies.

### (c) NMR Experiments

The conformational analysis of *epiCF<sub>3</sub>QD* in CDCl<sub>3</sub> and DMSO-*d*<sub>6</sub> was achieved via NOESY and HOESY with a concentration of 15 mM at 298 K, and the corresponding conformational distribution was determined by <sup>1</sup>H NMR and <sup>19</sup>F NMR peak integrations. To determine the *syn-anti* conformational distribution of *epiCF<sub>3</sub>QD* in other solvents, we initially focused on the assignment of <sup>19</sup>F NMR signals. In most non-alcoholic solvents, the <sup>19</sup>F NMR signal corresponding to the *syn* conformations appeared downfield to that of the *anti* conformations (Figure 2-C and 2-D). In alcohols and water, the <sup>19</sup>F NMR signal of the *syn* conformations appeared upfield. The assignment could be verified by adding CHCl<sub>3</sub> or DMSO into a particular solvent, which led to increase or decrease of the *syn* population, respectively. When deuterated solvents were used, the population distribution could also be measured based on the H9 signals of the *syn* and *anti* conformations in the <sup>1</sup>H NMR, whose relative chemical shifts did not vary with solvent. Using these methods, the *syn-anti* conformational distribution of *epiCF<sub>3</sub>QD* in 47 solvents was determined via <sup>19</sup>F NMR peak integrations.<sup>17a</sup> The Open-Closed conformational equilibria of QD and *epiQD* in various solvents were derived

based on <sup>3</sup>J<sub>H8H9</sub> coupling constants, which were measured in the corresponding solvents with a concentration of 15 mM at 298 K.

## 2. Result and Discussion

### 2.1 Investigation of the Conformations of Quinidine Derivatives via Quantum Chemical Calculations

Figure 1-E illustrates the most stable conformers of *epiCF<sub>3</sub>QD* in local minima on the PES (See SI for all 21 conformers). The relative energies of fully optimized conformers differ from those indicated on the PES due to different computational methods.

At the B3LYP/6-311+G(d,p) level of theory, seven conformers were identified on the PES of *epiQD* (Figure 1-C). Taking the  $\tau_3$  rotation into consideration, the number of conformers increased to 13, and the most stable species of conformers 1-7 are shown in Figure 1-F (See SI for all 13 conformers). Because of the structural resemblance of QD to cinchonidine (CD), the conformers of QD could be identified with the help of the PES of CD (Figure 1-D).<sup>9d</sup> By including the  $\tau_3$  rotation into the conformer exploration, 19 conformers were found (Open-11 was not found), and the minimum-energy species of conformers 1-10 are shown in Figure 1-G.

As depicted in Figure 1-B, C and D, *epiCF<sub>3</sub>QD*, *epiQD*, and QD were found to share several similar patterns on their PESs. First, seven major conformers, Closed-1, Closed-2, Open-3, Open-4 (Open-9 for *epiCF<sub>3</sub>QD*), Open-5, Open-6, and Closed-7, were distributed at relatively similar locations on the PESs of these three molecules, implying their analogous conformational behavior (Figure 1-B-D). Second, high barriers to  $\tau_2$  rotation have been observed in all three cases, which lead to the kinetic categorization of conformers into two groups, namely, the *syn*- and the *anti*-conformations. This was particularly important for the conformational study of *epiCF<sub>3</sub>QD*, as it led to two NMR distinguishable signals responsible for the *syn*- and the *anti*-conformers at room temperature, respectively. The direct measurement of the *syn-anti* conformational equilibrium could thus be achieved through NMR peak integration.<sup>17</sup> Third, barriers to the  $\tau_1$  rotations were generally found in the range of a few kcal/mol. With such low rotational barriers, signals of all *syn* (or *anti*) conformers of *epiCF<sub>3</sub>QD* can coalesce into a single peak in the <sup>19</sup>F NMR spectrum, therefore significantly streamlining signal assignment and conformational analysis.

Apart from these similarities, noticeable differences in conformational distributions were also observed. On the PES of QD, only two minima, Open-3 and Open-4, were found in the zone of  $\tau_1$  ational distrFigure 1-D). In comparison, the same region in the PES of *epiCF<sub>3</sub>QD* proved more intricate. Three additional conformers were identified as Open-4, Open-8 and Open-10, corresponding to eclipsed geometry along the C8-C9 bond. Presumably, the energetic cost for forming these seemingly unfavorable conformers is largely reduced by the formation of intramolecular H-bonding and the avoidance of steric interactions between the CF<sub>3</sub> group and the quinoline ring. Compared with the scattered conformational distribution in the region of  $\tau_1$  group and the quinoline ring. Compared with the scattered conformationaregion for *epiCF<sub>3</sub>QD*. This is presumably due to steric interactions between the CF<sub>3</sub> group and the H18 atom. *epiQD* was found to be conformationally less diverse than QD and *epiCF<sub>3</sub>QD* (Figure 1-C). This can be ascribed to (a) significant stabilization of Open-3 and Open-4 via intramolecular H-bonding (compared with QD) and (b) less steric congestion around the C8-C9 bond in Open-3 and Open-4 (compared with *epiCF<sub>3</sub>QD*). Noticeably, while the conformational distribution of *epiQD* is restricted due to high thermodynamic stabilities of Open-3 and Open-4 conformers compared with others, PES of *epiQD* was found to be kinetically shallow, which allows a conformational exchange faster than *epiCF<sub>3</sub>QD*.



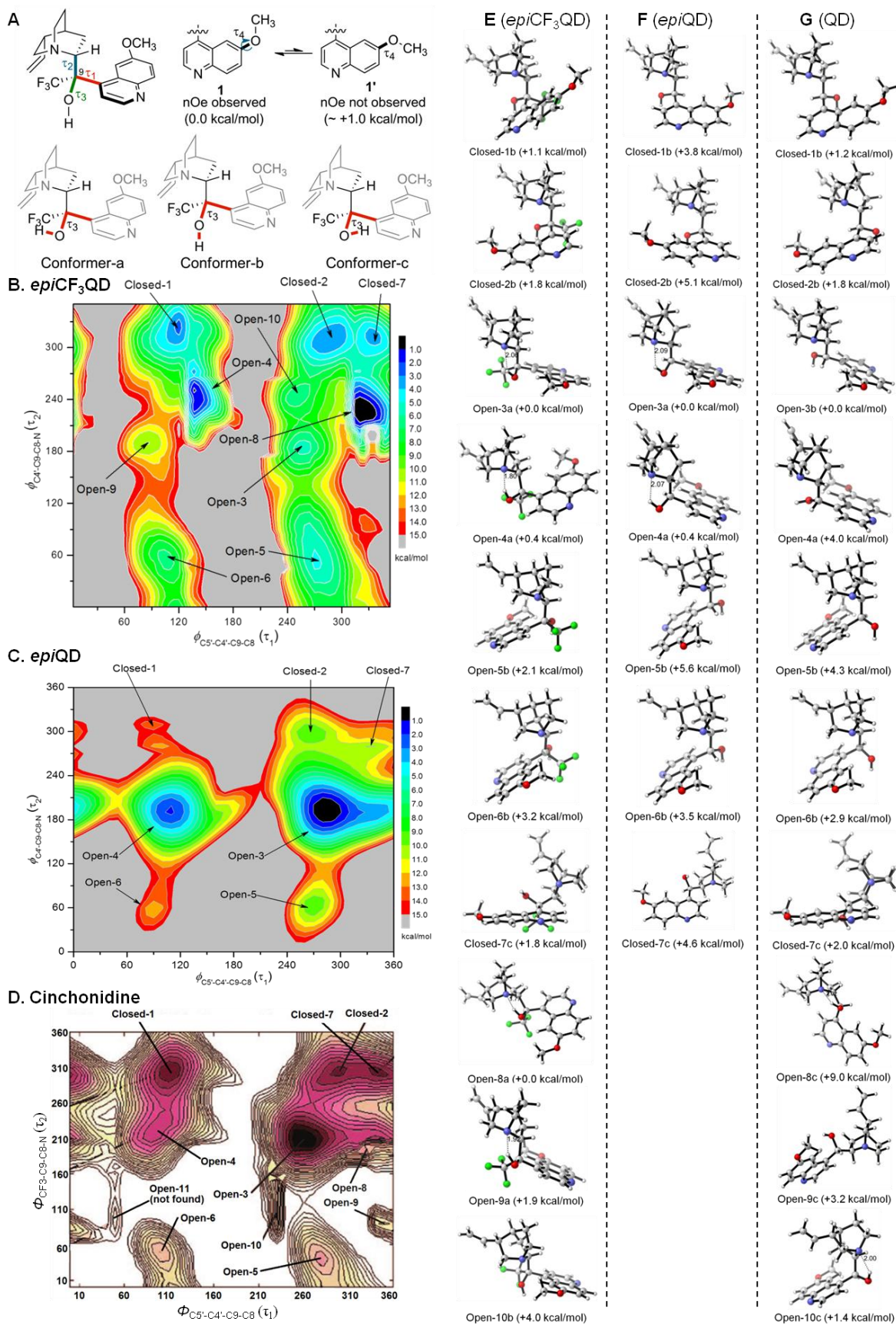


**Figure 1.** A. Critical rotations in conformational analysis; B-D. PES of *epiCF<sub>3</sub>QD*, *epiQD*, and cinchonidine<sup>9d</sup> in the gas phase, respectively; Figure 1-D was reprinted with permission from Ref. 9d. Copyright (2008) American Chemical Society. E-G. Representative conformers of *epiCF<sub>3</sub>QD*, *epiQD*, and QD in the gas phase; Relative Gibbs free energies (gas phase) are shown in parentheses.

## 2.2 Conformational Behavior of *epiCF<sub>3</sub>*QD

### 2.2.1 Conformational Study of *epiCF<sub>3</sub>*QD via <sup>19</sup>F NMR

By introducing the CF<sub>3</sub> group into quinidine, the conformational equilibrium around  $\tau_2$ , namely the *syn-anti* equilibrium could be investigated in various solvents. According to NOESY spectroscopy, the major species of *epiCF<sub>3</sub>*QD in CDCl<sub>3</sub> were Open-3-like (*syn*) conformations, while the minor species adopted Open-4-like (*anti*) geometry (Figure 2-A).<sup>17</sup> This result is similar to the above-mentioned calculations in the gas phase. The relative populations of these two species were determined to be 83:17 by <sup>19</sup>F NMR integrations, respectively. In DMSO, the Closed-1 and the Closed-2 conformations were adopted with a 50:50 ratio (Figure 2-B).

Representative results have been shown in Figures 2-C, 2-D, and Table 1. In general, high *syn:anti* ratios were seen in solvents possessing low dielectric constants ( $\epsilon$ ), such as pentane ( $\epsilon = 1.84$ ), benzene ( $\epsilon = 2.27$ ), and CHCl<sub>3</sub> ( $\epsilon = 4.89$ ). In contrast, significant stabilization of *anti* conformation was found in solvents with relatively high  $\epsilon$ , such as acetone ( $\epsilon = 21.0$ ), acetonitrile ( $\epsilon = 36.6$ ), and DMSO ( $\epsilon = 47.2$ ). This trend is consistent with both our theoretical calculations (See Table S22) and previous observations<sup>3,5,7a</sup> which showed an Onsager-type inverse correlation between the population of Open-3-like conformations and  $\epsilon$  of solvents.

Apart from the agreement of experimental results with calculations, noticeable differences were also observed. Nitrobenzene and nitromethane are “highly polar” solvents based on their dielectric constants ( $\epsilon = 35.6$  and  $\epsilon = 37.7$ , respectively). However, the population of *syn* conformations ( $Pop_{syn,exp}$ ) of *epiCF<sub>3</sub>*QD in these two solvents was found to be fairly high (78% and 82%, respectively), which is essentially the same as the  $Pop_{syn,exp}$  in “non-polar” solvent toluene ( $\epsilon = 2.28$ ,  $Pop_{syn,exp} = 82\%$ , Figure 2-C, spectrum 3, Figure 2-D, spectra 3 and 4). Despite the fact that water is among the most polar solvent on the dielectric constant polarity scale ( $\epsilon = 80.8$ ), a relatively high  $Pop_{syn,exp}$  (71%) was observed. Moreover, according to dielectric constants, the conformational behavior of *epiCF<sub>3</sub>*QD in THF ( $\epsilon = 7.52$ ) and pyridine ( $\epsilon = 10.4$ ) was expected to be similar to that in CH<sub>2</sub>Cl<sub>2</sub> ( $\epsilon = 8.93$ ). Instead, dramatically different conformational distributions were found, as  $Pop_{syn,exp} = 65\%$  in THF,  $Pop_{syn,exp} = 83\%$  in CH<sub>2</sub>Cl<sub>2</sub>, and  $Pop_{syn,exp} = 53\%$  in pyridine. These exceptional results clearly indicate certain deficiencies of dielectric polarity in describing solvent-solute interactions involving *epiCF<sub>3</sub>*QD. In other words, specific interactions, such as H-bonding, may influence the conformational behavior of cinchona alkaloids. It is worth noting that the possible effects of specific interactions were also noticed by Bürgi and Baiker;<sup>5</sup> however, a clear mechanistic rationale was not achieved due to the paucity of related data.

### 2.2.2. Elucidation of Solvent Effects Based on Linear Free Energy Relationship (LFER)

LFER has been successfully utilized in elucidating complicated chemical processes and interactions, such as asymmetric catalysis<sup>25</sup> and solvent-solute interactions.<sup>26b,27</sup> In principle, the establishment of a good linear relationship with a solvent polarity scale indicates the predominance of the corresponding solvent-solute interaction in a chemical process or equilibrium. A systematic exploration of solvent effects on the *syn-anti* equilibrium of *epiCF<sub>3</sub>*QD was performed by means of LFER.<sup>26</sup> To examine the accuracy of the previously proposed Onsager function<sup>28</sup> in predicting cinchona alkaloid conformational distribution,<sup>5</sup> we attempted to establish a linear correlation of  $\Delta G_{syn,exp}$  with  $(\epsilon-1)/(\epsilon+2)$  (denoted by  $Y$ ).<sup>29</sup> However, only a weak correlation ( $R^2 = 0.351$ ) was obtained with 39 data points (Figure 3-C, Table 2, see SI for details), therefore excluding electrostatic interaction as the dominant solvent effect influencing the *syn-anti* equilibrium. Plotting the previously reported  $\Delta G_{open-3}$  of CD<sup>5,30</sup> against  $(\epsilon-1)/(\epsilon+2)$

led to a similarly weak correlation ( $R^2 = 0.361$ ). Both of these results are in agreement with the notion that specific interactions can significantly influence the conformational behavior of cinchona alkaloids and their derivatives (See SI for details).

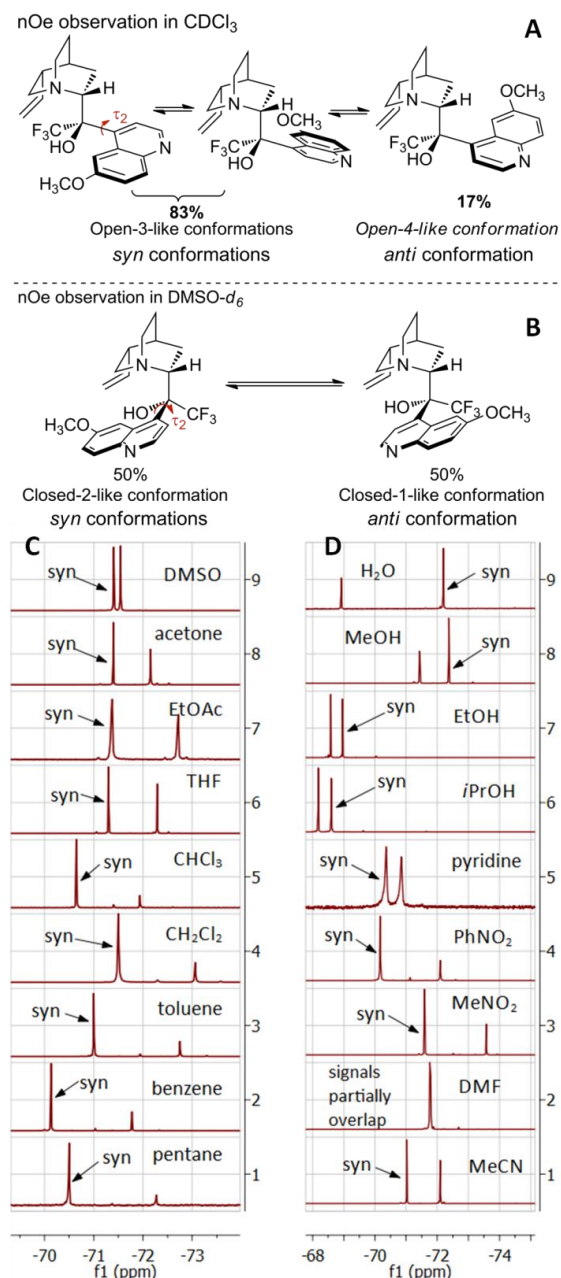


**Figure 2.** A. Observed conformational distribution of *epiCF<sub>3</sub>*QD in CDCl<sub>3</sub>; B. Observed conformational distribution of *epiCF<sub>3</sub>*QD in DMSO-*d*<sub>6</sub>; C.-D. <sup>19</sup>F NMR spectrum of *epiCF<sub>3</sub>*QD in various solvents (See SI, Tables S22 and S23 for complete data).

To describe the complicated solvent effects, a multiparameter approach, incorporating both specific and nonspecific aspects of solvation by means of linear combination, is necessary.<sup>26b,27b,31</sup> In particular, H-bonding interactions are expected to be significant due to the presence of the quinoline/quinuclidine and the hydroxyl functionalities. Based on this analysis, the multiparameter expression should be composed of at least four independent parameters, namely, (a) the polarization term  $(\epsilon-1)/(\epsilon+2)$  (reflects electrostatic interaction,  $Y$ ),<sup>26b</sup> (b) the polarizability term  $(n^2-1)/(n^2+2)$  (reflects



London's dispersive force, denoted by  $P$ ,<sup>26b</sup> and (c and d) the H-bond donating and accepting ability  $\alpha$  and  $\beta$ .<sup>32</sup>

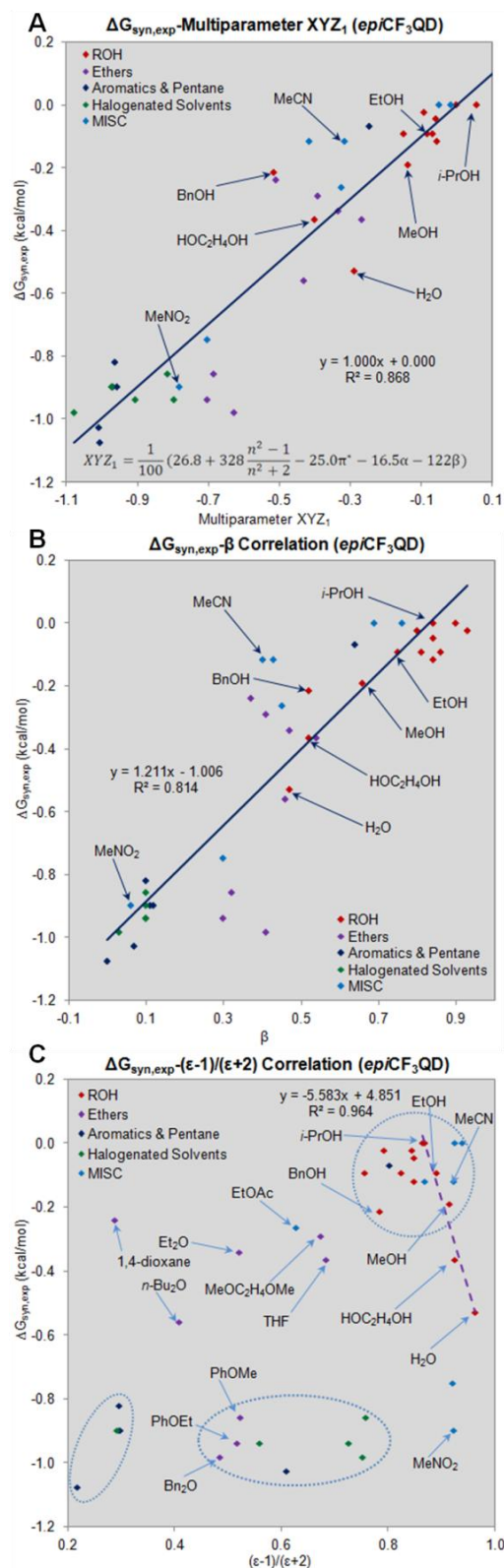


**Figure 3.** A. Correlation of  $\Delta G_{\text{syn,exp}}$  of  $\text{epiCF}_3\text{QD}$  with multiparameter polarity scale  $\text{XYZ}_1$ ; B. Correlation of  $\Delta G_{\text{syn,exp}}$  of  $\text{epiCF}_3\text{QD}$  with H-bond accepting ability ( $\beta$ ) of various solvents; C. Plot of  $\Delta G_{\text{syn,exp}}$  of  $\text{epiCF}_3\text{QD}$  versus  $(\epsilon-1)/(\epsilon+2)$  of various solvents (dielectric interaction).

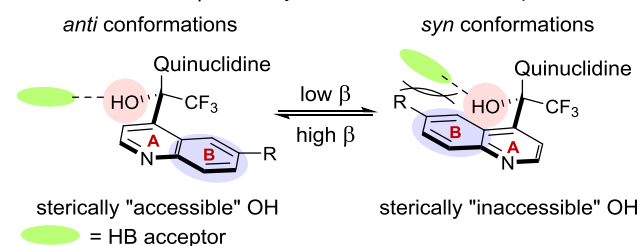
Since overall nonspecific solvent-solute interactions can be approximated by the empirical polarity scale  $\pi^*$  (primarily a blend of  $Y$  and  $P$ ) with a polarizability correction term  $p \cdot (n^2-1)/(n^2+2)$ ,<sup>33</sup> a multiparameter polarity scale was devised as

$$\text{XYZ} = \text{XYZ}_0 + a \cdot \alpha + b \cdot \beta + s \cdot \pi^* + p \cdot P,$$

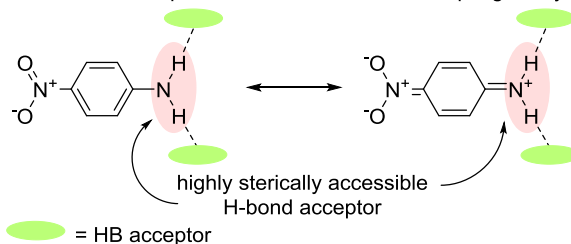
where  $\text{XYZ}_0$ ,  $a$ ,  $b$ ,  $s$ , and  $p$  are solvent independent regression coefficients and indicative of the sensitivity of the conformational equilibrium toward the corresponding solvent property.

This equation resembles the well-known Kamlet-Taft expression.<sup>32</sup> In comparison, the quality of  $\text{XYZ}$ , the  $\text{XYZ}'$  ( $\text{XYZ}' = \text{XYZ}_0 + a \cdot \alpha + b \cdot \beta + y \cdot Y + p \cdot P$ ) scale and the empirical polarity scale  $E_T^N$ <sup>35</sup> were also investigated. On the  $\text{XYZ}$  scale, the nonspecific polarity term  $s \cdot \pi^* + p \cdot P$  accounts for solvation induced by solvent dipoles, quadruples, higher multipoles and dispersive forces. On the  $\text{XYZ}'$  scale, because the nonspecific polarity term  $y \cdot Y + p \cdot P$  can only describe dipolar and dispersive interactions, the  $\text{XYZ}'$  scale differs from the  $\text{XYZ}$  scale mainly by the absence of quadrupolar and higher multipolar interactions.<sup>33b</sup>

#### A. Plausible role of $\beta$ in the *syn-anti* conformational equilibrium



#### B. Solvatochromic probe for solvent H-bond accepting ability $\beta$



#### C. Steric effect of solvents on conformational distribution

Example 1:

	PhOMe, PhOEt, (PhCH <sub>2</sub> ) <sub>2</sub> O	<i>n</i> -Bu <sub>2</sub> O	Et <sub>2</sub> O, 1,4-dioxane, MeOC <sub>2</sub> H <sub>4</sub> OMe, THF
$\beta$	0.30–0.41	0.46	0.37–0.54
$\Delta G_{\text{syn,exp}}$ (kcal/mol)	-0.86 - -0.98	-0.56	-0.24 - -0.37
steric hindrance around the O atom decreases			

Example 2:

	Me≡N:	Me-C(=O)-Me	Me-C(=O)-OMe	Me-O-Me
$\beta$	0.40	0.43	0.45	0.47
$\Delta G_{\text{syn,exp}}$ (kcal/mol)	-0.12	-0.12	-0.27	-0.34
steric hindrance around the HB accepting site increases				

**Figure 4.** A. Plausible role of H-bonding interaction in the *syn-anti* conformational equilibrium; B. Determination of H-bond accepting ability ( $\beta$ ) using solvatochromic probe, in which the H-bond acceptor possesses less steric encumbrance than the hydroxyl group in  $\text{epiCF}_3\text{QD}$ ; C. Steric effect of solvents on the conformational distribution.  $\Delta G_{\text{syn,exp}}$  varies significantly with relatively unchanged  $\beta$  values, revealing that the steric hindrance around solvents' HB accepting sites can influence the conformational distribution of  $\text{epiCF}_3\text{QD}$ .

**Table 1. LFER Analysis of Solvent Effects on the Conformational Behavior of Quinidine and Its Derivatives.**

polarity scale	interacting mechanism	correlation coefficient ( $R^2$ )			
		<i>epi</i> CF <sub>3</sub> QD		QD	
		syn-anti equilibrium		open-closed equilibrium	
		$\Delta G_{\text{syn,exp}}$ (39 solv.)	$\Delta G_{\text{syn,cal}}$ (18 solv.)	$\Delta G_{\text{open,exp}}$ (18 solv.)	$\Delta G_{\text{open,cal}}$ (18 solv.)
$(\epsilon-1)/(\epsilon+2)$ , $Y$	electrostatic interaction (nonspecific, polarization)	0.350	0.975	0.088	0.998
$(n^2-1)/(n^2+2)$ , $P$	dispersive interaction (nonspecific, polarizability)	0.237	-	0.017	-
$\pi^*$	nonspecific van der Waals interactions (primarily a linear combination of $Y$ and $P$ )	0.001	-	0.466	-
$\alpha$	H-bond donating ability (specific)	0.304	-	0.012	-
$\beta$	H-bond accepting ability (specific)	0.814	-	0.120	-
$E_T^N$	nonspecific van der Waals and specific H-bonding interactions (an approximate linear combination of $\pi^*$ , $\alpha$ and $\beta$ )	0.317	-	0.029	-
XYZ	a linear combination of $P$ , $\pi^*$ , $\alpha$ and $\beta$	0.868	-	0.872	-
XYZ'	a linear combination of $Y$ , $P$ , $\alpha$ and $\beta$	0.861	-	0.554	-

Table 1 and Figure 3-A show a good linearity between  $\Delta G_{\text{syn,exp}}$  and the XYZ<sub>1</sub> polarity scale ( $R^2 = 0.868$ ). A good correlation was also obtained with the XYZ<sub>1</sub>' scale, which excludes effects induced by solvent quadrupoles and higher multipoles. In contrast,  $\Delta G_{\text{syn,exp}}$  was found to weakly correlate with  $E_T^N$  ( $R^2 = 0.317$ , see SI for details). In spite of the weak dependence of  $\Delta G_{\text{syn,exp}}$  with single parameters  $Y$ ,  $P$ ,  $\pi^*$ , and  $\alpha$ , the H-bond accepting ability of solvents ( $\beta$ ) was found to well correlate to  $\Delta G_{\text{syn,exp}}$  ( $R^2 = 0.814$ ). The coefficient of the  $\Delta G_{\text{syn,exp}}-\beta$  correlation was essentially the same as that of the  $\Delta G_{\text{syn,exp}}-\text{XYZ}$  correlation, revealing the predominance of the H-bond accepting ability of solvents in overall solvent effects (Figure 3-B).

The positive correlation of  $\Delta G_{\text{syn,exp}}$  with  $\beta$  in Figure 3-B indicates that the *syn* conformations are stabilized in solvents with low  $\beta$  values. This observation can be explained by the different steric environments around the hydroxyl group in the *syn* and the *anti* conformations (Figure 4-A). In the *syn* conformations, the hydroxyl group is sterically insulated by the quinoline ring and thus less involved in H-bonding interaction. In contrast, the hydroxyl group in the *anti* conformation is an effective H-bond donor due to its higher accessibility. The H-bonding thus tends to stabilize *anti* conformations more than its *syn* counterparts. In general, hydrocarbon-based solvents and their halogenated derivatives are poor H-bonding acceptors. Neither *syn* nor *anti* conformations are stabilized in these solvents through specific interactions; this results in large energy differences as observed in the gas phase (ca. -1.0 kcal/mol). Some ethers, such as diethyl ether (Et<sub>2</sub>O), di-*n*-butyl ether (*n*-Bu<sub>2</sub>O), and THF, possess moderate H-bond acceptance, thus leading to moderate  $\Delta G_{\text{syn,exp}}$  values by stabilizing *anti* conformations (ca. -0.4 kcal/mol). Such  $\Delta G_{\text{syn,exp}}-\beta$  correlation was particularly strong in protic solvents, *i.e.* H<sub>2</sub>O, ethylene glycol, MeOH, EtOH and *i*-PrOH (Figure 3-B).

Apart from these good linear relationships, noticeable deviations of  $\Delta G_{\text{syn,exp}}$  from the  $\beta$ -scale were also observed. For example, according to  $\beta$  values, all ethers of interest possess similar H-bond accepting abilities ( $0.30 < \beta < 0.54$ ); nevertheless, significantly higher  $\Delta G_{\text{syn,exp}}$  values were observed in aromatic ethers than in saturated ethers (Figure 4-C, Example 1). Since the  $\beta$ -scale was derived based on the H-bonding interaction of sterically "non-hindered" *p*-nitroaniline (and other structurally similar probes), the steric effects of H-bond acceptors on  $\beta$  values should be minimal (Figure 4-B). In comparison, the hydroxyl group in *epi*CF<sub>3</sub>QD is located in a rather crowded environment. Its H-bonding interaction with ethers is expected to decrease as the steric hindrance around the ethereal oxygen atom increases (aro-

matic ether > *n*-Bu<sub>2</sub>O > other ethers). Similarly, although acetonitrile, acetone, ethyl acetate, and Et<sub>2</sub>O have similar  $\beta$  values, their stabilizing effects on the *anti* conformations were found to gradually decrease with the increase in the steric encumbrance around the H-bond accepting site (Figure 4-C, Example 2).

It is worth noting that the importance of H-bonding interactions on the conformational equilibrium of *epi*CF<sub>3</sub>QD can also be inferred by the conformational behavior of its *O*-methylated derivatives (*epi*MeOCF<sub>3</sub>QD)<sup>17b</sup>. <sup>19</sup>F NMR spectroscopy shows that the *syn* population of *epi*MeOCF<sub>3</sub>QD is almost constant (>95%) in solvents with various  $\beta$  values (See SI for details). Such an observation may be attributed to both the steric congestion around the C9 atom and the absence of the OH-solvent specific interactions, which govern the conformational behavior of *epi*CF<sub>3</sub>QD.

Regarding the  $\Delta G_{\text{syn,exp}}-(\epsilon-1)/(\epsilon+2)$  correlation, the most significant data scattering was found in the moderate polarity region ( $0.3 < (\epsilon-1)/(\epsilon+2) < 0.7$ ). We ascribed this observation to the incapability of  $(\epsilon-1)/(\epsilon+2)$  in describing steric effects and H-bond accepting ability. For example, although the introduction of C-NO<sub>2</sub> and C-Cl dipolar moieties can increase the  $\epsilon$  of many solvents, these moieties are weak H-bonding acceptors. Such mismatching thus leads to significant deviation in  $\Delta G_{\text{syn,exp}}-(\epsilon-1)/(\epsilon+2)$  correlation in halogenated and nitro-containing solvents.

In contrast, a close association of  $\Delta G_{\text{syn,exp}}$  with dielectric constant polarity was found in solvents possessing high or low  $\epsilon$  values. Large  $\Delta G_{\text{syn,exp}}$  (ca. -1.0 – -0.8 kcal/mol) values were commonly observed in solvents with  $(\epsilon-1)/(\epsilon+2)$  values < 0.3, whereas  $\Delta G_{\text{syn,exp}}$  became rather small (ca. 0.0 – -0.3 kcal/mol) with high  $(\epsilon-1)/(\epsilon+2)$  values (> 0.7). Although this trend appears in good agreement with the previous conclusion by Bürgi and Baiker, such consistency may just simply be due to the positive interrelation between the  $\beta$  and the  $\epsilon$  scales. Strong H-bond accepting ability generally necessitates significant charge separation within solvent molecules (such as DMSO and DMF), which in turn leads to high  $\epsilon$  values. On the other hand, solvents containing no dipolar moieties, such as hydrocarbons, usually have both low dielectric constants and weak H-bond accepting ability.

Good linearity ( $R^2 = 0.964$ ) was established between  $\Delta G_{\text{syn,exp}}$  and  $(\epsilon-1)/(\epsilon+2)$  in the family of simple alcohols (water, ethylene glycol, MeOH, EtOH, *n*-PrOH and *i*-PrOH), as  $\Delta G_{\text{syn,exp}}$  decreased with the increase in dielectric constant. Moreover, a strong negative correlation ( $R^2 = 0.969$ ) was also found between  $\beta$  and  $(\epsilon-1)/(\epsilon+2)$  of simple alcohols. Gas phase calculations have shown that binding energies of aniline (as a donor) with water, MeOH, EtOH and *n*-PrOH (as acceptors) are essentially the same;



namely, their “intrinsic” H-bond accepting abilities are identical (See SI for details). This implies that the different empirical H-bond accepting abilities ( $\beta$ ) of these alcohols mainly originate from their dielectric constants rather than the strength of the O-H bond. In other words, with increased dielectric constant, an alcoholic solvent tends to solvate itself more strongly via dipolar interaction, therefore leading to the decrease in their H-bond acceptance to *epiCF<sub>3</sub>QD*. Due to practically the same “intrinsic” H-bond accepting abilities of simple alcohols, solvation energies of the *syn* and the *anti* conformers in these solvents are anticipated to primarily correlate with  $(\epsilon-1)/(\epsilon+2)$ . This result shows that the Onsager function is applicable only in cases where the influence of other interactions is similar or negligible.

### 2.2.3 Comparison of Theoretical Calculations with Experimental Data

Based on the DFT calculations mentioned in 2.1.2,  $\Delta G_{\text{syn,cal}}$  of *epiCF<sub>3</sub>QD* obtained in 18 solvents was plotted against the corresponding  $\Delta G_{\text{syn,exp}}$ , which yielded a correlation with a  $R^2$  value of 0.381 (Figure 5-A, red line). On the other hand, although the PCM model exploits a formalization different from that of the simple Onsager model to calculate solvent effects,<sup>22</sup>  $\Delta G_{\text{syn,cal}}$  was found to be strongly correlated to the Onsager-like function  $(\epsilon-1)/(\epsilon+2)$  ( $R^2 = 0.967$ ) only with small deviation. Because of this, the weak correlation between  $\Delta G_{\text{syn,exp}}$  and  $\Delta G_{\text{syn,cal}}$  can be ascribed to the inconsistency of  $(\epsilon-1)/(\epsilon+2)$  with  $\beta$ , as confirmed by the resemblance of the  $\beta-(\epsilon-1)/(\epsilon+2)$  plot to the  $\Delta G_{\text{syn,exp}}-\Delta G_{\text{syn,cal}}$  plot (through a clockwise rotation of 180°, Figure 5-A has very similar pattern as Figure 5-C). As depicted,  $\Delta G_{\text{syn,exp}}$  and  $\Delta G_{\text{syn,cal}}$  significantly diverged when  $\beta$  and  $(\epsilon-1)/(\epsilon+2)$  values are “mismatched” (Figure 5-A and 5-C, red spots without circles).

Noticeably, even though  $\Delta G_{\text{syn,exp}}$  and  $(\epsilon-1)/(\epsilon+2)$  were found to be positively correlated in alcohols (See SI for details), theory predicted an opposite solvent-dependence trend (Figure 5-B). In our PCM-based calculations, *epiCF<sub>3</sub>QD* predominantly interacts with the solvent through an Onsager-type behavior. This may differ from the actual solvation, in which the H-bonded *epiCF<sub>3</sub>QD*-alcohol complexes (or alcohol solvent shell) interact with solvent molecules through an interaction similar to Onsager-type description, which can probably explain the opposite predication of solvent effects.

### 2.3 Conformational Behavior of *epiQD* in Various Solvents

As mentioned in 2.1, DFT calculations have provided the  $\Delta G_{\text{open,cal}}$  of 13 *epiQD* conformers in the gas phase. Two major conformers were identified in the gas phase, as Open-3a and Open-4a, with relative energies of 0.0 and 0.4 kcal/mol, respectively (Table 2). Other than these two species, all other conformers are energetically unfavorable ( $\Delta G > 3.5$  kcal/mol). Similar to *epiCF<sub>3</sub>QD*, the intramolecular quinuclidine-N $\cdots$ H-O H-bonding has been found in Open-3a and Open-4a as indicated by the short N-H contacts. According to second order perturbation theory analysis,<sup>24</sup> the donor (lone pair on N)-acceptor ( $\sigma_{\text{O-H}}^*$ ) interaction energies are around 0.5 kcal/mol or less, which are significantly weaker than the internal H-bonding in Open-3a of *epiCF<sub>3</sub>QD* (5.7 kcal/mol). Because the N $\cdots$ H distances and N $\cdots$ H-O bond angles in *epiQD* conformers are close to the corresponding values in Open-3a of *epiCF<sub>3</sub>QD*, the significantly smaller interaction energy can be attributed to the weaker acidity of the OH group in *epiQD*.

As shown in Table 3, the population summation of Open-3 and Open-4 was calculated to be >99.6% in solvents under investigation, and the  $\Delta G_{\text{open-3}}$  was obtained based on the corresponding  $\text{Pop}_{\text{open-3}}/\text{Pop}_{\text{open-4}}$  values. Plotting the  $\Delta G_{\text{open-3}}$  against  $(\epsilon-1)/(\epsilon+2)$  led to a rather high linearity ( $R^2 = 1.000$ ), which resembles the Onsager function.<sup>28</sup> To quantify the population distribution of *epiQD* in different solvents, we adopted a method described by

Baiker *et al.*,<sup>5</sup> which assumed the observed  $J_{\text{H8H9}}$  to be a weighted averaged coupling constant of all conformers, namely  $\text{caPop}_{(i)} \times J_{\text{H8H9}(i)}$ . Moreover, with calculated H8-C9-C8-H9 dihedral angles ( $\phi_{\text{H8H9}(i)}$ ) in hand, the corresponding vicinal coupling constants ( $J_{\text{H8H9}(i)}$ ) of different conformers (i) were obtained via a modified Karplus equation,<sup>36</sup> in which both substituent and stereochemistry effects are taken into consideration.

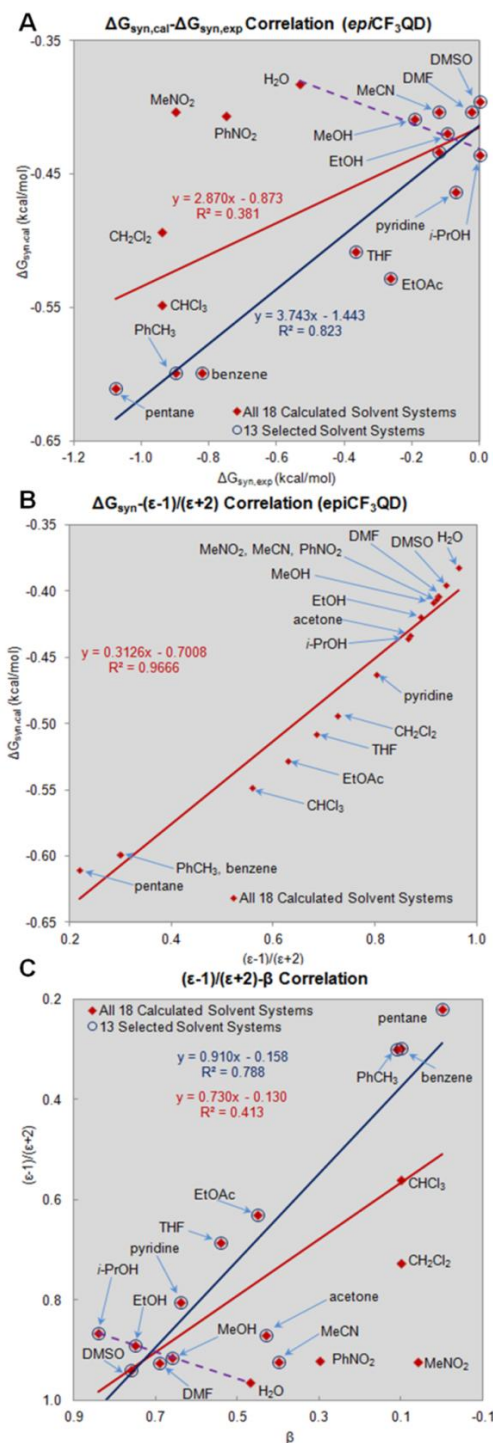


**Figure 5.** A. Correlation of  $\Delta G_{\text{syn,exp}}$  of *epiCF<sub>3</sub>QD* with  $\Delta G_{\text{syn,cal}}$ ; five uncircled calculated  $\Delta G_{\text{syn,cal}}$  values significantly diverge from the experimental data; B. Correlation of  $\Delta G_{\text{syn,cal}}$  of *epiCF<sub>3</sub>QD* with  $(\epsilon-1)/(\epsilon+2)$  of various solvents (dipolar interaction); C. Correlation of  $(\epsilon-1)/(\epsilon+2)$  with  $\beta$ , which shows a scattered pattern similar to Figure 5-A.

**Table 2. Calculated Properties of Different Conformers of *epi*QD in the Gas Phase.<sup>a</sup>**

Conformer	$\Delta G$ (kcal/mol) <sup>b</sup>	$Pop$ (%) <sup>c</sup>	$\phi_{H8H9}$ <sup>d</sup>	$J_{H8H9}$ (Hz) <sup>e</sup>	$J_{H8H9} \times Pop$ (Hz) <sup>f</sup>
Closed-1a	5.6	0.0	299.4	3.41	0.0
Closed-1b	3.8	0.1	299.0	3.36	0.0
Closed-2b	5.1	0.0	293.9	2.80	0.0
Closed-7c	4.6	0.0	290.1	2.41	0.0
Open-3a	0.0	67.8	185.3	8.81	6.0
Open-3b	4.7	0.0	169.5	8.40	0.0
Open-4a	0.4	31.9	184.8	8.84	2.8
Open-4b	4.9	0.0	165.6	8.02	0.0
Open-4c	8.6	0.0	165.6	8.02	0.0
Open-6a	4.9	0.0	60.1	3.47	0.0
Open-6b	3.5	0.2	60.3	3.45	0.0
Open-5a	7.5	0.0	62.8	3.71	0.0
Open-5b	5.6	0.0	60.0	3.48	0.0

<sup>a</sup> Calculated at the M06-2X/6-311+G(d,p)//B3LYP/6-311+G(d,p) level; <sup>b</sup> relative Gibbs Free Energies ( $\Delta G$ ) to Open-3a; <sup>c</sup> population ( $Pop$ ); <sup>d</sup> dihedral angle of H<sub>8</sub>-C<sub>9</sub>-C<sub>8</sub>-H<sub>9</sub> ( $\phi_{H8H9}$ ); <sup>e</sup> predicted  $J_{H8H9}$  based on modified Karplus equation; <sup>f</sup> the coupling constant contribution of each conformer to the overall  $J_{H8H9}$ .

**Table 3. PCM-Based Calculated Conformational Distribution of *epi*QD in Various Solvents.<sup>a</sup>**

solvent	$Pop_{open-3} / Pop_{open-4}$ (%/%) <sup>a,b</sup>	$\Delta G_{open-3}$ (kcal/mol) <sup>a</sup>	$J_{H8H9,cal}$ (Hz) <sup>c</sup>	$J_{H8H9,exp}$ (Hz) <sup>d</sup>
benzene	61.9/37.8	-0.29	8.8	9.8
toluene	-	-	-	9.8
CHCl <sub>3</sub>	57.5/42.3	-0.18	8.8	9.8
CH <sub>2</sub> Cl <sub>2</sub>	-	-	-	9.9
THF	55.4/44.3	-0.13	8.8	9.7
<i>i</i> -PrOH	-	-	-	9.8
acetone	-	-	-	9.8
EtOH	-	-	-	9.4
MeOH	51.4/48.3	-0.03	8.8	9.3
PhNO <sub>2</sub>	-	-	-	9.8
MeCN	51.3/48.4	-0.03	8.8	9.5
MeNO <sub>2</sub>	-	-	-	9.9
DMF	-	-	-	9.8
DMSO	51.0/48.7	-0.02	8.8	9.0
H <sub>2</sub> O	50.5/49.1	-0.01	8.8	9.3

<sup>a</sup> Calculated at the PCM-M06-2X/6-311+G(d,p)//B3LYP/6-311+G(d,p) level of theory; <sup>b</sup> according to the calculation, Open-3 and Open-4 were found to be the major conformers, and the overall population of other conformers ranges from 0.2-0.4% in various solvents; <sup>c</sup> predicted  $J_{H8H9}$  based on modified Karplus equation and calculated dihedral angle of H<sub>8</sub>-C<sub>9</sub>-C<sub>8</sub>-H<sub>9</sub> ( $\phi_{H8H9}$ ); <sup>d</sup> measured by <sup>1</sup>H NMR (500 MHz) in deuterated solvents.

Given the facts that the observed  $J_{H8H9}$  was almost constant in all solvents and Open-3 and Open-4 had essentially the same  $J_{H8H9}$ , these two gas phase abundant conformers should be dominant in all solvents. This result is in good agreement with our calculated coupling constant, in which  $J_{H8H9}$  was shown to be solvent-independent (Table 3). Hence, it can be concluded that conformers with  $\Delta G > 3.5$  kcal/mol in the gas phase were unlikely to be significantly populated in solution. The NOESY of *epi*QD in CD<sub>2</sub>Cl<sub>2</sub> and DMSO-*d*<sub>6</sub> also identified both Open-3 and Open-4 as major conformers with very similar correlation patterns, revealing that the  $Pop_{open-3}/Pop_{open-4}$  ratio did not change significantly in different solvents (See SI for details). According to the gas phase calculations at the B3LYP/6-311+G(d,p) level, Open-3 and Open-

4 possessed very similar dipole moments (5.20 and 5.42 D, respectively). Thus the dipolar interaction on the conformational equilibrium should be insignificant.

## 2.4 Conformational Behavior of QD in Various Solvents

QD is conformationally more flexible than *epi*QD. This is not only reflected by its higher number of conformers (19 minimum energy conformers were found for QD), but also by its shallower PES in the gas phase (Table 4). Compared with *epi*QD, which only had two conformers possessing  $\Delta G < 3.0$  kcal/mol, eight conformers were found for QD within that energy range. Similar to cinchonidine,<sup>5,9d</sup> Open-3b, Closed-1b, Closed-2b, Closed-7c, and Open-10c were identified to be important conformers with population higher than 2%. Differing from *epi*CF<sub>3</sub>QD and *epi*QD, the stereochemistry of QD does not allow the formation of internal H-bonding in its Open-3 conformation (Figure 1-G). Instead, sterically unfavorable Open-10c was found to be stabilized by internal H-bonding, which provides a stabilization of 3.0 kcal/mol as indicated by the second order perturbation theory NBO analysis.<sup>24</sup>

**Table 4. Calculated Properties of Different Conformers of QD in the Gas Phase.<sup>a</sup>**

Conformer	$\Delta G_{cal}$ (kcal/mol) <sup>b</sup>	$Pop$ (%) <sup>c</sup>	$\phi_{H8H9}$ <sup>d</sup>	$J_{H8H9}$ (Hz) <sup>e</sup>	$J_{H8H9} \times Pop$ (Hz) <sup>f</sup>
Closed-1a	3.1	0.4	175.4	9.15	0.0
Closed-1b	1.2	9.2	173.3	9.13	0.8
Closed-2a	3.3	0.3	175.6	9.15	0.0
Closed-2b	1.8	3.6	176.0	9.15	0.3
Closed-7a	4.1	0.1	179.8	9.11	0.0
Closed-7b	2.4	1.3	178.9	9.13	0.1
Closed-7c	2.0	2.6	179.6	9.11	0.2
Open-3b	0.0	74.4	78.3	0.95	0.7
Open-3c	2.3	1.7	82.5	0.92	0.0
Open-4a	4.0	0.1	60.2	1.89	0.0
Open-4b	3.1	0.4	80.7	0.92	0.0
Open-9b	3.3	0.3	80.4	0.92	0.0
Open-9c	3.2	0.3	81.3	0.92	0.0
Open-5b	4.3	0.1	281.4	1.38	0.0
Open-6a	4.7	0.0	293.8	2.27	0.0
Open-6b	2.9	0.5	287.2	1.73	0.0
Open-6c	3.5	0.2	315.3	4.58	0.0
Open-8c	9.0	0.0	316.6	4.72	0.0
Open-10c	1.4	6.5	317.1	4.78	0.3

<sup>a</sup> Calculated at the M06-2X/6-311+G(d,p)//B3LYP/6-311+G(d,p) level of theory; <sup>b</sup> relative Gibbs Free Energies ( $\Delta G_{cal}$ ) to Open-3b; <sup>c</sup> relative population ( $Pop$ ); <sup>d</sup> dihedral angle of H<sub>8</sub>-C<sub>9</sub>-C<sub>8</sub>-H<sub>9</sub> ( $\phi_{H8H9}$ ); <sup>e</sup> predicted  $J_{H8H9}$  obtained via modified Karplus equation; <sup>f</sup> the coupling constant contribution of each conformer to the overall  $J_{H8H9}$ .

$\Delta G_{open,cal}$  in various solvents was calculated based on the overall population of Open conformations, *i.e.* Open-3~8 and Open-8~10. The  $\Delta G_{open,cal}$  of QD was found to perfectly correlate with  $(\epsilon-1)/(\epsilon+2)$  of 13 solvents with  $R^2 = 0.998$  (Figure 6-B). The population of Open-3b significantly decreases with the increase in  $\epsilon$  of solvents, while the population of closed conformers generally increases in solvents with high dielectric constant. This result could be ascribed to the relatively lower dipole moment of Open-3b ( $\mu = 2.65$  D in the gas phase) compared with other conformers ( $\mu > 3.12$  D in the gas phase).

**Table 5. Conformational Distribution of QD and  $\Delta G_{\text{open,exp}}$  in Various Solvents.**

solvent	$J_{\text{H8H9,exp}}$ (Hz) <sup>a,b</sup>	$\text{Pop}_{\text{open,exp}}$ (%) <sup>c</sup>	$\Delta G_{\text{open,exp}}$ (kcal/mol) <sup>d</sup>	$\Delta G_{\text{open,cal}}$ (kcal/mol) <sup>e</sup>
dioxane	4.3	59	-0.21	-
benzene	3.9	64	-0.34	-0.56
<i>p</i> -xylene	3.4	70	-0.49	-
PhCl	4.4	58	-0.18	-
THF	4.9	52	-0.04	-0.0
<i>o</i> -C <sub>6</sub> H <sub>4</sub> Cl <sub>2</sub>	4.9	52	-0.04	-
ClC <sub>2</sub> H <sub>4</sub> Cl	5.4	46	0.10	-
pyridine	4.9	52	-0.04	0.18
<i>i</i> -PrOH	2.0	87	-1.12	0.28
acetone	5.4	46	0.10	0.29
EtOD	2.5	81	-0.88	0.36
MeOD	2.8	77	-0.71	0.35
PhNO <sub>2</sub>	5.4	46	0.10	0.38
MeCN	7.8	16	0.97	0.38
MeNO <sub>2</sub>	7.3	22	0.74	0.38
DMF	4.9	52	-0.04	0.38
DMSO	4.9	52	-0.04	0.40
H <sub>2</sub> O	7.3	22	0.74	0.45

<sup>a</sup> Observed  $J_{\text{H8H9}}$ , measured by <sup>1</sup>H NMR (500 MHz) in deuterated solvents as indicated; <sup>b</sup> significant line broadening of the H<sub>8</sub> signal (d) was observed in many cases, which leads to difficulty in the determination of  $J_{\text{H8H9,exp}}$ . Under such circumstance,  $J_{\text{H8H9,exp}}$  was achieved by measuring the coupling constant of the doublet of the H<sub>9</sub> signal (td); <sup>c</sup> population of Open-conformations achieved based on  $J_{\text{H8H9,exp}}$  and modified Karplus equation; <sup>d</sup> derived based on the Boltzmann equation and  $\text{Pop}_{\text{open,exp}}$  data; <sup>e</sup>  $\Delta G_{\text{open,cal}} = -RT \ln(T \text{Pop}_{\text{open}} / \sum \text{Pop}_{\text{closed}})$

To quantify the population distribution of QD in solvents via  $J_{\text{H8H9}}$  analysis, we adopted the two-equation-two-variable linear system described by Baiker *et al.*<sup>5</sup> As the Closed conformations had essentially the same coupling constant, the linear system involved two equations and at least three variables,  $\text{Pop}_{\text{Open-3}}$ ,  $\text{Pop}_{\text{Closed}}$ , and  $\text{Pop}_{\text{Open-10}}$  (Eq. 3 and 4).

$$J_{\text{H8H9}}^{\text{obs}} = J_{\text{H8H9}}^{\text{Open-3}} \times \text{Pop}_{\text{Open-3}} + J_{\text{H8H9}}^{\text{Closed}} \times \text{Pop}_{\text{Closed}} + J_{\text{H8H9}}^{\text{Open-10}} \times \text{Pop}_{\text{Open-10}} \quad \text{Eq. 3}$$

$$\text{Pop}_{\text{Open-3}} + \text{Pop}_{\text{Closed}} + \text{Pop}_{\text{Open-10}} = 1 \quad \text{Eq. 4}$$

where  $J_{\text{H8H9}}^{\text{obs}}$  is the observed  $J_{\text{H8H9}}$ ;  $J_{\text{H8H9}}^{\text{Open-3}}$ ,  $J_{\text{H8H9}}^{\text{Closed}}$  and  $J_{\text{H8H9}}^{\text{Open-10}}$  are  $J_{\text{H8H9}}$  of Open-3, Closed and Open-10 conformations, respectively.  $\text{Pop}_{\text{Open-3}}$ ,  $\text{Pop}_{\text{Closed}}$  and  $\text{Pop}_{\text{Open-10}}$  are populations of Open-3, Closed and Open-10 conformers, respectively.

According to NOESY spectrum, Open-10c was not a major conformer in solution, which was consistent with both the present and the previous PCM calculations.<sup>9d</sup> Moreover, it was anticipated that the population of Open-10c could further decrease because of diminishing internal H-bonding in H-bond accepting solvents. Therefore, with moderate  $J_{\text{H8H9}}$  values and low population, Open-10c was estimated to have negligible influence on the observed vicinal couplings (< 0.5 Hz). The exclusion of the contribution from Open-10c thus led to systematic errors in conformational distribution quantification, which did not significantly affect the trend of solvent dependence. On this basis, a two-equation-two-variable linear system similar to the previous expression<sup>5</sup> was formulated (Eq. 1 and Eq. 2), which allowed the determination of

$(\text{Pop}_{\text{Open}}/\text{Pop}_{\text{Closed}})_{\text{exp}}$  via  $J_{\text{H8H9}}$  analysis (Table 5).  $\Delta G_{\text{open,exp}}$  in 18 solvents was thus obtained.

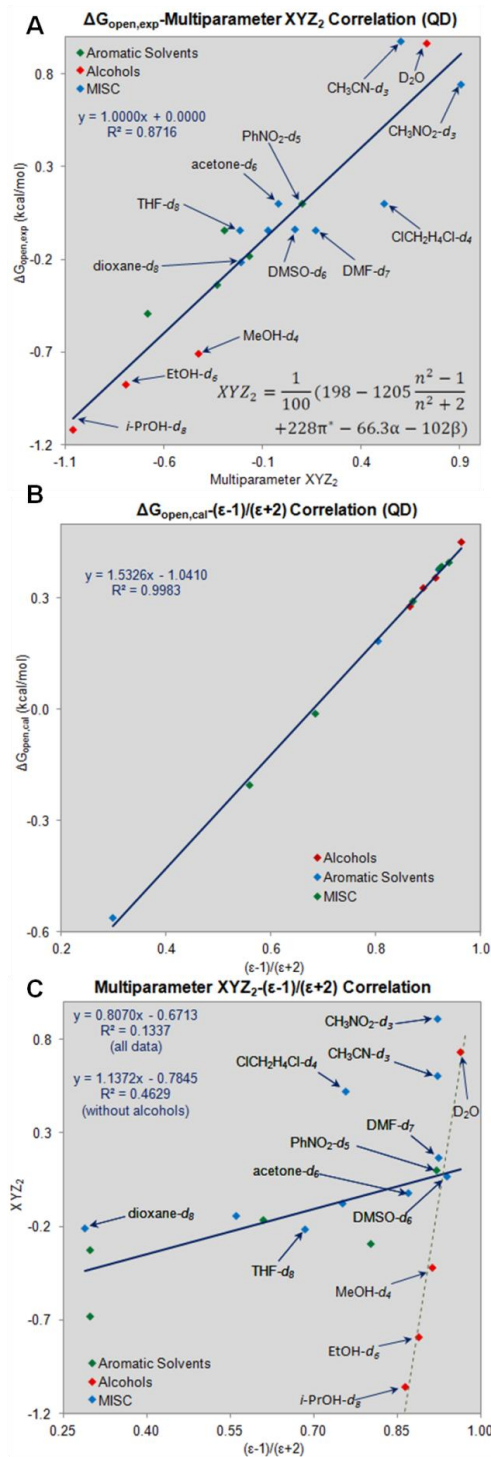


**Figure 6.** A. Correlation of  $\Delta G_{\text{open,exp}}$  with multiparameter XYZ<sub>2</sub>; B. Correlation of  $\Delta G_{\text{open,cal}}$  of QD with ( $\epsilon-1$ )/( $\epsilon+2$ ) of various solvents (dielectric interaction); C. Correlation of multiparameter XYZ<sub>2</sub> with ( $\epsilon-1$ )/( $\epsilon+2$ ).

Even though  $\Delta G_{\text{open,exp}}$  was almost independent on ( $\epsilon-1$ )/( $\epsilon+2$ ) ( $R^2 = 0.088$ , Table 1), a good correlation was found within the family of alcoholic solvents. As discussed in Section 2.2.3, such an observation can be presumably rationalized by the similar contribution from the specific solvent-solute interactions to the overall solvation energy.

On the other hand, a good linear relationship of  $\Delta G_{\text{open,exp}}$  was established with multiparameter  $\text{XYZ}_2$ , which was a linear combination of  $\alpha$ ,  $\beta$ ,  $\pi^*$ , and a polarizability correction term  $p \cdot P$  ( $R^2 = 0.872$ ) (Figure 6-A, Table 2). In contrast, the multiparameter  $\text{XYZ}_2'$ , namely  $\text{XYZ}_0' + y \cdot Y + p \cdot P + a \cdot \alpha + b \cdot \beta$ , correlated with  $\Delta G_{\text{open,exp}}$  to give a relatively lower  $R^2 = 0.554$ . The poorer correlation is presumably owing to the absence of significant quadrupole and higher multipole terms. To assess the reliability of PCM-based calculations,  $\text{XYZ}_2$  was plotted against  $(\epsilon-1)/(\epsilon+2)$  to yield a very weak correlation (Figure 6-C). Evidently, *the present PCM calculations, practically resembling the Onsager function, is not sufficiently accurate to describe the overall solvation of QD, which involves interacting mechanisms other than dielectric interaction.*

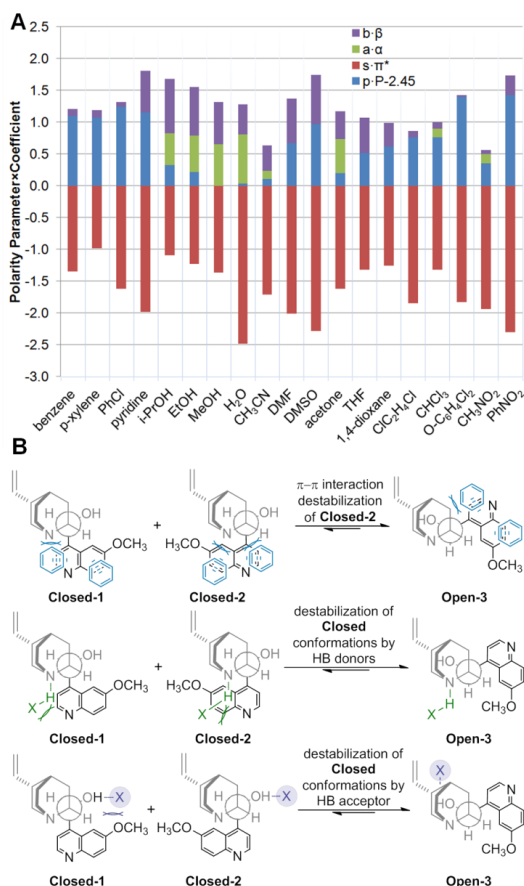


**Figure 7.** A. Contribution from individual solvent properties to the multiparameter  $\text{XYZ}_2$ ;  $\alpha$  and  $\beta$  represent H-bond donating ability, respectively.  $\pi^*$  describes nonspecific van der Waals interactions. B. Rationalization of stabilization/destabilization from solvent-solute interactions.

Figure 7-A demonstrates the contribution from individual polarity parameter to the multiparameter  $\text{XYZ}_2$ . According to the large values of  $s \cdot \pi^*$  terms, aromatic solvents were as “polar” as other solvents, such as  $\text{CH}_3\text{CN}$  and  $\text{CH}_3\text{NO}_2$ , thus leading to the expectation of large  $\Delta G_{\text{open}}$ . However, the high  $\pi^*$  polarity of aromatic solvents was largely compensated for polarizability correction term  $p \cdot P$  (Figure 7-A, notice the significant blue bars ( $p \cdot P$ ) of aromatic solvents compared with the small  $p \cdot P$  values of  $\text{CH}_3\text{CN}$  and  $\text{CH}_3\text{NO}_2$ ). This implies that the Open conformations (mainly Open-3) were stabilized by dispersive interaction (Figure 7-B).<sup>37</sup> Such effects were particularly notable for the conformational equilibrium in  $\text{CH}_3\text{NO}_2$  and  $\text{PhNO}_2$ , as  $\text{Pop}_{\text{open}}$  was found doubled in the latter (Table 6). The overall H-bonding interaction was approximately the same in  $\text{H}_2\text{O}$  and in alcohols (notice purple

bars and green bars of alcohols in Figure 7-A). Therefore, the significant destabilization of Open conformations in  $\text{H}_2\text{O}$ , compared with other alcohols, is primarily due to nonspecific interactions (notice red bars of alcohols in Figure 7-A).

Based on the multiparameter dissection, it is also obvious that the exceptionally high  $\text{Pop}_{\text{open}}$  in alcohols is due to both H-bond accepting and donating capacity of the solvents, which cancels out the effects due to other nonspecific van der Waals interactions ( $s \cdot \pi^* + p \cdot P$ ). Similar to the observation with *epi*CF<sub>3</sub>QD, the H-bond accepting ability of solvents was also found to stabilize the *anti* conformations of QD (Open-3, Figure 3-B). The relatively weak impact of  $\beta$  on the conformational equilibrium of QD is in part due to the lower acidity of the OH group and the absence of intramolecular H-bonding in major conformers. The stabilization of Open conformations by H-bonding donation from solvents can be rationalized by the higher accessibility of the quinuclidine nitrogen in the respective conformations (Figure 3-B).

### 3. The Influence of Solvent-Induced Conformational Behavior of QD in $\text{S}_{\text{N}}2$ Reaction, A Case Study.

As mentioned above, the links between the conformation and the catalytic activity/reactivity of cinchona alkaloids have been well documented in the literature.<sup>1f,3-9</sup> Herein, a model  $\text{S}_{\text{N}}2$  reaction, as an additional example to other well-known studies, is presented to address the influence of solvent-induced conformational change of QD on its reactivity toward  $\alpha$ -bromoacetate (Figure 8-A). Similar  $\text{S}_{\text{N}}2$  reactions have been shown to be critical for many catalytic and synthetic processes, such as Gaunt's enantioselective catalytic cyclopropanation reaction<sup>38</sup> and the synthesis of various cinchona alkaloid-based phase-transfer catalysts.<sup>1f</sup>

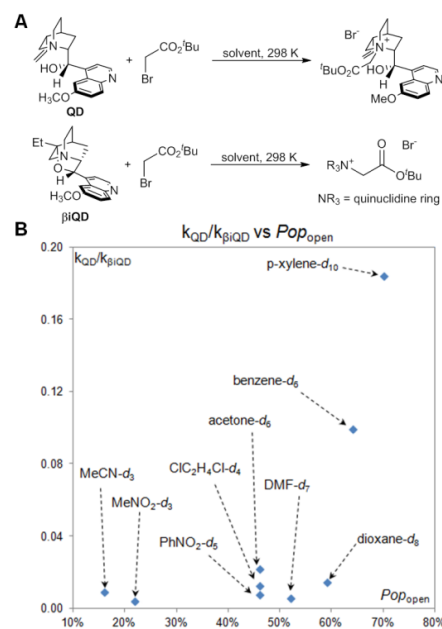


**Figure 8.** A. Reactions between quinidine/ $\beta$ -isoquinidine and  $\alpha$ -bromoacetate; B. The influence of population of Open-conformations of quinidine on reaction rates.  $k_{\text{QD}}$  and  $k_{\beta\text{IQD}}$  are the rate constant of the reaction of QD and  $\beta$ IQD with  $\alpha$ -bromoacetate, respectively.  $\text{Pop}_{\text{open}}$  is the population of open-conformations in the corresponding solvent. See Table 5.

As the rate of  $\text{S}_{\text{N}}2$  reactions can be significantly affected by solvent polarity even in the absence of conformational changes,<sup>34</sup>  $\beta$ -isoquinidine ( $\beta$ IQD), which only adopts Open-conformations, was exploited to account for such types of solvent effects.<sup>40a</sup> By



comparing the relative rate constant of the reaction with QD ( $k_{\text{QD}}/k_{\beta\text{QD}}$ ) in different solvents, the role of conformations in reaction kinetics can be inferred. Figure 8-B shows a plot of  $k_{\text{QD}}/k_{\beta\text{QD}}$  as a function of the population of Open-conformations of QD ( $\text{Pop}_{\text{open}}$ ) in various solvents. Although the relationship is not linear, a noticeable trend can be seen as the relative reaction rate constant,  $k_{\text{QD}}/k_{\beta\text{QD}}$ , increases with the increase of  $\text{Pop}_{\text{open}}$  (See SI for details). In line with the notably higher reaction rate constant with  $\beta\text{iQD}$  than that with QD, the observed trend implies that the Open-conformations are likely to be more reactive than the Closed-conformations, which presumably can be attributed to the reduced steric hindrance around the reactive quinuclidine-*N* atom in Open-conformations.<sup>40b</sup>

## Conclusions

By incorporating a trifluoromethyl group in the C9 carbon of quinuclidine, the conformational exchange can be significantly decelerated to allow the direct determination of the conformational distribution in various solvents. With these results, the reliability of the PCM model-based theoretical calculation was assessed, which demonstrated considerable divergence from the experimental data. These errors in theoretical calculations are mainly due to the complicated solvent-cinchona alkaloids interaction mechanism that cannot be fully described by the PCM model. In fact, only the conformers with calculated Gibbs free energies higher than 3.5 kcal/mol in the gas phase can be excluded as populated species in solution. Based on the present results and Baiker's seminal two-equation-two-variable linear system, the Open-Closed conformational equilibria in various solvents were determined. It was found that the previous correlation of the Open-3 population of cinchona alkaloids with the dielectric constant of solvents was in fact unsuccessful. Instead, the LFER analysis using multiparameter polarity scales has been proven to be a powerful tool for quantitative prediction of solvent effects on the conformational behavior of cinchona alkaloids and their derivatives. The importance of solvent-induced conformational distributions was demonstrated in a case study of the  $\text{S}_{\text{N}}2$  reaction between QD and  $\alpha$ -bromoacetate, which suggests a higher reactivity of open-conformations compared to closed-conformations. Overall this reveals a complicated solvent-solute interaction scenario involving both nonspecific and specific forces.

## ASSOCIATED CONTENT

### Supporting Information

Experimental procedures, calculation details, analytical data, and NMR spectra. This material is available free of charge via the Internet at <http://pubs.acs.org>.

## AUTHOR INFORMATION

### Corresponding Author

gprakash@usc.edu

### Notes

The authors declare no competing financial interests.

## ACKNOWLEDGMENTS

Financial support for our work by the Loker Hydrocarbon Research Institute is greatly acknowledged. Prof. T. Williams is gratefully thanked for his valuable suggestions and discussions on the manuscript. The computational studies were supported by the University of Southern California Center for High-Performance Computing and Communications. Mr. J.-P. Jones is acknowledged for providing additional computational resources.

## REFERENCES

- (1) (a) Kolb, H. C.; VanNieuwenhze, M. S.; Sharpless, K. B. *Chem. Rev.* **1994**, *94*, 2483-2547. (b) O'Donnell, M. J. *Acc. Chem. Res.* **2004**, *37*, 506-517. (c) Chen, Y.; McDaid, P.; Deng, L. *Chem. Rev.* **2003**, *103*, 2965-2983. (d) France, S.; Guerin, D. J.; Miller, S. J.; Lectka, T. *Chem. Rev.* **2003**, *103*, 2985-3012. (e) Yoon, T. P.; Jacobsen, E. N. *Science* **2003**, *299*, 1691-1693. (f) Song, C. E. Ed. *Cinchona Alkaloids in Synthesis and Catalysis*; Wiley-VCH: Weinheim, **2009**.
- (2) For discussions on conformational effects on chemical reactivity, J. I. Seeman, *Chem. Rev.* **1983**, *83*, 84-134.
- (3) (a) Hiemstra, H.; Wynberg, H. *J. Am. Chem. Soc.* **1981**, *103*, 417-430. (b) Dijkstra, G. D. H.; Kellogg, R. M.; Wynberg, H.; Svendsen, J. S.; Marko, I.; Sharpless, K. B. *J. Am. Chem. Soc.* **1989**, *111*, 8069-8076. (c) Svendsen, J. S.; Markó, I. E.; Jacobsen, E. N.; Pulla Rao, C.; Bott, S.; Sharpless, K. B. *J. Org. Chem.* **1989**, *54*, 2263-2664.
- (4) (a) Corey, E. J.; Noe, M. C. *J. Am. Chem. Soc.* **1993**, *115*, 12579-12580. (b) Corey, E. J.; Noe, M. C.; Sarshar, S. *Tetrahedron Lett.* **1994**, *35*, 2861-2864. (c) Corey, E. J.; Noe, M. C. *J. Am. Chem. Soc.* **1996**, *118*, 319-329. (d) Li, H.; Liu, X.; Wu, F.; Tang, L.; Deng, L. *Proc. Natl. Acad. Sci. USA* **2010**, *107*, 20625-20629.
- (5) Bürgi, T.; Baiker, A. *J. Am. Chem. Soc.* **1998**, *120*, 12920-12926.
- (6) (a) Bucher, C.; Mondelli, C.; Baiker, A.; Gilmour, R. *J. Mol. Catal. A: Chem.* **2010**, *327*, 87-91. (b) Zimmer, L. E.; Sparr, C.; Gilmour, R. *Angew. Chem. Int. Ed.* **2011**, *50*, 11860-11871. (c) Schmidt, E.; Bucher, C.; Santarossa, G.; Mallat, T.; Gilmour, R.; Baiker, A. *J. Catal.* **2012**, *289*, 238-248. (d) Tanzer, E.-M.; Schweizer, W. B.; Ebert, M.-O.; Gilmour, R. *Chem. Eur. J.* **2012**, *18*, 2006-2013.
- (7) (a) Aune, M.; Matsson, O. *J. Org. Chem.* **1995**, *60*, 1356-1364. (b) Busygin, I.; Nieminen, V.; Taskinen, A.; Sinkkonen, J.; Toukonitty, E.; Sillanpää, R.; Murzin, D. Yu.; Leino, R. *J. Org. Chem.* **2008**, *73*, 6559-6569.
- (8) (a) Vayner, G.; Houk, K. N.; Sun, Y.-K. *J. Am. Chem. Soc.* **2004**, *126*, 199-203, and references therein. (b) A. Vargas, T. Bürgi, A. Baiker, *J. Catal.* **2004**, *226*, 69-82. (c) Çelebi-Ölçüm, N.; Aviñente, V.; Houk, K. N. *J. Org. Chem.* **2009**, *74*, 6944-6952.
- (9) (a) Ferri, D.; Bürgi, T.; Baiker, A. *J. Chem. Soc., Perkin Trans. 2* **1999**, 1305-1311. (b) Ferri, D.; Bürgi, T.; Borszeky, K.; Mallat, T.; Baiker, A. *J. Catal.* **2000**, *193*, 139-144. (c) Meier, D. M.; Urakawa, A.; Turrà, N.; Rüegger, H.; Baiker, A. *J. Phys. Chem. A* **2008**, *112*, 6150-6158. (d) Urakawa, A.; Meier, D. M.; Rüegger, H.; Baiker, A. *J. Phys. Chem. A* **2008**, *112*, 7250-7255. (e) Bürgi, T.; Vargas, A.; Baiker, A. *J. Chem. Soc., Perkin Trans. 2*, **2002**, *9*, 1596-1601.
- (10) Olsen, R. A.; Borchardt, D.; Mink, L.; Agarwal, A.; Mueller, L. J.; Zaera, F. *J. Am. Chem. Soc.* **2006**, *128*, 15594-15595.
- (11) Karle, J. M.; Bhattacharjee, A. K. *Bioorg. Med. Chem.* **1999**, *7*, 1769-1774.
- (12) (a) Prelog, V.; Wilhelm, M. *Helv. Chim. Acta* **1954**, *37*, 1634-1660. (b) Dijkstra, G. D. H.; Kellogg, R. M.; Wynberg, H. *J. Org. Chem.* **1990**, *55*, 6121-6131.
- (13) For recent discussion on PCM models, Mennucci, B. *J. Phys. Chem. Lett.* **2010**, *1*, 1666-1674.
- (14) Karplus, M. *J. Chem. Phys.* **1959**, *30*, 11-15.
- (15) Neuhaus, D.; Williamson, M. P. *The Nuclear Overhauser Effect in Structural and Conformational Analysis*, 2nd ed.; John Wiley & Sons: New York, **2000**, pp 321-322 and 391-398.

- (16) Discussions on steric effects of the trifluoromethyl group, (a) Schlosser, M.; Michel, D. *Tetrahedron* **1996**, 52, 99-108. (b) Uneyama, K. *Organofluorine Chemistry*; Blackwell Publish: Oxford, **2006**, pp 82-83. (c) Charton, M. *J. Am. Chem. Soc.* **1975**, 97, 1552-1556.
- (17) (a) Prakash, G. K. S.; Wang, F.; Ni, C.; Shen, J.; Haiges, R.; Yudin, A. K.; Mathew, T.; Olah, G. A. *J. Am. Chem. Soc.* **2011**, 133, 9992-9995. (b) Prakash, G. K. S.; Wang, F.; Rahm, M.; Shen, J.; Ni, C.; Haiges, R.; Olah, G. A. *Angew. Chem. Int. Ed.* **2011**, 50, 11761-11764.
- (18) A comprehensive book describing  $^{19}\text{F}$  NMR spectroscopy, see: Dolbier, Jr. W. R. *Guide to Fluorine NMR for Organic Chemists*; John Wiley and Sons: New Jersey, **2009**, pp 4-5.
- (19) Gaussian 09, Revision B.01, Frisch, M. J.; Trucks, G. W.; Schlegel, H. B.; Scuseria, G. E.; Robb, M. A.; Cheeseman, J. R.; Scalmani, G.; Barone, V.; Mennucci, B.; Petersson, G. A.; Nakatsuji, H.; Caricato, M.; Li, X.; Hratchian, H. P.; Izmaylov, A. F.; Bloino, J.; Zheng, G.; Sonnenberg, J. L.; Hada, M.; Ehara, M.; Toyota, K.; Fukuda, R.; Hasegawa, J.; Ishida, M.; Nakajima, T.; Honda, Y.; Kitao, O.; Nakai, H.; Vreven, T.; Montgomery, Jr., J. A.; Peralta, J. E.; Ogliaro, F.; Bearpark, M.; Heyd, J. J.; Brothers, E.; Kudin, K. N.; Staroverov, V. N.; Kobayashi, R.; Normand, J.; Raghavachari, K.; Rendell, A.; Burant, J. C.; Iyengar, S. S.; Tomasi, J.; Cossi, M.; Rega, N.; Millam, N. J.; Klene, M.; Knox, J. E.; Cross, J. B.; Bakken, V.; Adamo, C.; Jaramillo, J.; Gomperts, R.; Stratmann, R. E.; Yazyev, O.; Austin, A. J.; Cammi, R.; Pomelli, C.; Ochterski, J. W.; Martin, R. L.; Morokuma, K.; Zakrzewski, V. G.; Voth, G. A.; Salvador, P.; Dannenberg, J. J.; Dapprich, S.; Daniels, A. D.; Farkas, Ö.; Foresman, J. B.; Ortiz, J. V.; Cioslowski, J.; Fox, D. J. Gaussian, Inc., Wallingford CT, 2009.
- (20) This computational approach was previously validated as a feasible estimation to the energetic and geometric properties of conformations with satisfactory accuracy, Hamza, A.; Schubert, G.; Soós, T.; Papai, I. *J. Am. Chem. Soc.* **2006**, 128, 13151.
- (21) Zhao, Y.; Truhlar, D. G. *Theor. Chem. Acc.* **2008**, 120, 215-241.
- (22) (a) Miertuš, S.; Scrocco, E.; Tomasi, J. *Chem. Phys.* **1981**, 55, 117-129. (b) Scalmani, G.; Frisch, M. J. *J. Chem. Phys.* **2010**, 132, 114110.
- (23) In this article, PCM is used as a synonym for IEFPCM.
- (24) (a) Reed, A. E.; Curtiss, L. A.; Weinhold, F. *Chem. Rev.* **1988**, 88, 899-926. (b) NBO Version 3.1, Glendening, E. D.; Reed, A. E.; Carpenter, J. E.; Weinhold, F..
- (25) For recent applications of LFER in mechanistic studies, (a) Jensen, K. H.; Sigman, M. S. *Angew. Chem. Int. Ed.* **2007**, 46, 4748-4750. (b) Baidya, M.; Kobayashi, S.; Brotzel, F.; Schmidhammer, U.; Riedle, E.; Mayr, H. *Angew. Chem. Int. Ed.* **2007**, 46, 6176-6179. (c) Sigman, M. S.; Miller, J. J. *J. Org. Chem.* **2009**, 74, 7633-7643. (d) Knowles, R. R.; Lin, S.; Jacobsen, E. N. *J. Am. Chem. Soc.* **2010**, 132, 5030-5032. (e) Jensen, K. H.; Sigman, M. S. *J. Org. Chem.* **2010**, 75, 7194-7201. (f) Li, X.; Deng, H.; Zhang, B.; Li, J.; Zhang, L.; Luo, Z.; Cheng, J.-P. *Chem. Eur. J.* **2010**, 16, 450-455. (g) Harper, K. C.; Sigman, M. S. *Proc. Natl. Acad. Sci. U.S.A.* **2011**, 108, 2179-2183. (h) Harper, K. C.; Sigman, M. S. *Science* **2011**, 333, 1875-1878. (i) Harper, K. C.; Bess, E. N.; Sigman, M. S. *Nat. Chem.* **2012**, 4, 366-374. (j) Gormisky, P. E.; White, M. C. *J. Am. Chem. Soc.* **2013**, 135, 14052-14055. (k) Prakash, G. K. S.; Zhang, Z.; Wang, F.; Rahm, M.; Ni, C.; Iulicucci, M.; Haiges, R.; Olah, G. A. *Chem. Eur. J.* **2014**, 20, 831-838.
- (26) (a) Wells, P. R. *Chem. Rev.* **1963**, 63, 171-219. (b) Koppel, I. A.; Palm, V. A. *Advances in Linear Free Energy Relationships*, Chapman, N. B. and Shorter, J. Ed., Plenum Press, London **1972**, pp 203-280.
- (27) (a) Reichardt, C. *Angew. Chem. Int. Ed. Engl.* **1979**, 18, 98-110. (b) Reichardt, C.; Welton, T. *Solvents and Solvent Effects in Organic Chemistry*, 4th Ed. Wiley-VCH: Weinheim, **2011**.
- (28) Onsager, L. *J. Am. Chem. Soc.* **1936**, 58, 1486-1493.
- (29) Approximate linear relationships have been found between various dielectric functions, including  $1/\epsilon$ ,  $(\epsilon-1)/(\epsilon+1)$ ,  $(\epsilon-1)/(\epsilon+2)$ ,  $(\epsilon-1)/(2\epsilon+1)$ . For example,  $(\epsilon-1)/(\epsilon+2)$  and  $(\epsilon-1)/(2\epsilon+1)$  has a correlation coefficient (R) of 0.978 and 0.991 when  $\epsilon \geq 1$  and 3, respectively. Therefore these dielectric functions are practically interchangeable. See reference 27(b), page 215-216.
- (30)  $\Delta G_{\text{open-3,exp}}$  of cinchonidine in various solvents was calculated based on the reported population ratio of Open-3 conformation and Closed conformations ( $\text{Pop}_{\text{Open-3,exp}}/\text{Pop}_{\text{Closed,exp}}$ ).
- (31) Selected reviews on multiparameter solvation models, (a) Katritzky, A. R.; Fara, D. C.; Yang, H.; Tamm, K. *Chem. Rev.* **2004**, 104, 175-198. (b) Marcus, Y. *Chem. Soc. Rev.* **1993**, 22, 409-416.
- (32) Kamlet, M. J.; Abboud, J.-L. M.; Abraham, M. H.; Taft, R. W. *J. Org. Chem.* **1983**, 48, 2877-2887.
- (33) (a) Abboud, J. L.; Kamlet, M. J.; Taft, R. W. *J. Am. Chem. Soc.* **1977**, 99, 8325-8327. (b) Laurence, C.; Nicolet, P.; Dalati, M. T.; Abboud, J. L. M.; Notario, R. J. *Phys. Chem.* **1994**, 98, 5807-5816.
- (34) Using original Kamlet-Taft solvent polarity expression ( $\text{XYZ}=\text{XYZ}_0+a\cdot\alpha+b\cdot\beta+s\cdot\pi+d\cdot\delta$ ),  $\Delta G_{\text{open,exp}}$  is correlated to multipolarity with  $R^2 = 0.705$ .  $\delta$  is a discontinuous polarizability correction term, which equals to 1.0, 0.5, and 0.0 for aromatic, polychlorinated, and all other aliphatic solvents, respectively.  $\delta$  possibly oversimplified the solvent effects. Reichardt, C.; Welton, T. *Solvents and Solvent Effects in Organic Chemistry*, 4th Ed. pp 497, Wiley-VCH: Weinheim, **2011**. In the present study, continuous polarizability  $P$ ,  $(n^2-1)/(n^2+1)$ , was found to be a better correction term.
- (35) Reichardt, C. *Chem. Rev.* **1994**, 94, 2319-2358.
- (36) Haasnoot, C. A. G.; DeLeeuw F. A. A. M.; Altona, C. *Tetrahedron* **1980**, 36, 2783-2792.
- (37) Cinchona alkaloids are known to form  $\pi$ - $\pi$  complexes at high concentrations in solution, (a) Uccello-Barretta, G.; Bari, L. D.; Salvadori, P. *Magn. Reson. Chem.* **1992**, 30, 1054-1063. (b) Marchettini, N.; Valensin, G.; Gaggelli, E. *J. Phys. Chem. A*, **2004**, 108, 8505-8513.
- (38) (a) Papageorgiou, C. D.; Ley, S. V.; Gaunt, M. J. *Angew. Chem. Int. Ed.* **2003**, 42, 828-831. (b) Bremeyer, N.; Smith, S. C.; Ley, S. V.; Gaunt, M. J. *Angew. Chem. Int. Ed.* **2004**, 43, 2681-2684. (c) Papageorgiou, C. D.; Cubilos de Dios, M. A.; Ley, S. V.; Gaunt, M. J. *Angew. Chem. Int. Ed.* **2004**, 43, 4641-4644. (d) Johansson, C. C. C.; Bremeyer, N.; Ley, S. V.; Owen, D. R.; Smith, S. C.; Gaunt, M. J. *Angew. Chem. Int. Ed.* **2006**, 45, 6024-6028. (e) A detailed mechanistic investigation on catalytically active conformations of cinchona alkaloid derivatives in Gaunt's cyclopropanation will be reported in due course.
- (39) Waldmann, H.; Khedkar, V.; Dücker, H.; Markus Schürmann, M.; Oppel, I. M.; Kumar, K. *Angew. Chem. Int. Ed.* **2008**, 47, 6869-6872.
- (40) (a) Solvent effects in the  $S_N2$  reaction of simple trialkylamine with alkyl halides, Abraham, M. H. *J. Chem. Soc. B*, **1971**, 299-308. (b) Our calculations at the PCM-M06-2X/6-311+G(d,p)//PCM-B3LYP/6-311+G(d,p) level of theory revealed that the barrier to the reaction between the Closed-2 conformation of *O*-methylated quinidine (MeOQD) and  $\alpha$ -bromoacetate in MeCN is ca. 2.0 kcal/mol higher than that of the Open-3 confor-

mation. These results are in good agreement with the current kinetic experiments and will be reported along with the study men-

tioned in reference 38(e).

## TOC

